



Research article

Radial phased-locked Laguerre-Gaussian correlated Schell-model beam array

Yaotian Yan, Guiqiu Wang^{**}, Yan Yin, Hongming Yin, Yaochuan Wang, Dajun Liu^{*}*Department of Physics, College of Science, Dalian Maritime University, Dalian, 116026, China*

ARTICLE INFO

Keywords:
 Propagation
 Beam array
 Partially coherent beam
 Laguerre-Gaussian correlation

ABSTRACT

A new beam array called radial phased-locked Laguerre-Gaussian correlated Schell-model (LGCSM) beam array is presented, the beamlet of this beam array is partially coherent beam with Laguerre Gaussian-Schell model correlation. The propagation expression of a radial phased-locked LGCSM beam array in free space is derived. It is aimed to give the effect of beam parameters on evolutions of beam array composed by LGCSM beam. The radial phased-locked LGCSM beam array has unique properties on propagation, the intensity of such beam array will evolve from a beam array composed of Gauss beams into a beam array formed of LGCSM beams. Furthermore, the intensity evolutions of such beam array are modulated by coherence length and beam order of beamlets. The obtained results are important in areas such as light field shaping, and free space optical communication.

1. Introduction

Recently, beam array has been widely studied due to its potential application in FSO and high-power laser system. The coherent laser beam arrays in turbulence have been analyzed [1, 2, 3, 4]. Partially coherent beams (PCBs) have widely been researched due to their advantages in turbulence [5], and models of beam array composed of PCBs are introduced. The properties of the beam array composed of the Gaussian Schell-model (GSM) beams are analyzed [6, 7, 8, 9, 10, 11]. In addition, new models of beam array are also introduced, such as random arrays [12], twist GSM array beams [13], radial phased-locked (PL) Lorentz beam array [14], radial PL rotating elliptical Gaussian beam array [15], radial PL partially coherent standard Hermite-Gaussian beam [16], radial PL partially coherent anomalous hollow beam array [17], radial PL partially coherent elegant Laguerre-Gaussian beam array [18], PL radially-polarized vector fields array [19], radial PL multi-GSM beam array [20], and rotating anisotropic GSM array beams [21]. Until now, most PCB arrays are related to GSM beams or multi-GSM beams. Thus, it is interesting to consider the beam array composed of a beam with a special correlation function. Recently, a new beam called Laguerre-Gaussian correlated Schell-model (LGCSM) beam has been proposed [22]. Henceforth, the evolutions of LGCSM vortex beam [23], twisted LGCSM beam [24], elliptical LGCSM beam with a twist [25], rectangular LGCSM beam [26, 27, 28], radially polarized LGCSM beam

[29], LGCSM with a twist phase [30], rotational elliptical LGCSM beam [31] are researched. From previous work, one can find that the dark hollow beam profile can be modulated by the parameters of LGCSM source on propagation. Hence, it gives a way to produce the beam array composed by dark hollow beam profile. It will be very interesting to consider the laser array composed by LGCSM beams, and the intensity of beam array can have linear, rectangular and radial distributions [14, 32, 33]. In this work, a new beam array called radial phased-locked LGCSM beam array is produced, which has M LGCSM beamlets. The cross-spectral density (CSD) of radial PL LGCSM beam array in free space is obtained, and the effects of beam parameters on evolution of a radial PL LGCSM beam array are discussed.

2. Analytical expression of an LGCSM beam array

At the source plane, the CSD for an elliptical LGCSM beam can be described as [22].

$$\Gamma(\mathbf{r}_1, \mathbf{r}_2, 0) = \exp\left(-\frac{\mathbf{r}_1^2 + \mathbf{r}_2^2}{4w_0^2}\right) \exp\left[-\frac{(x_2 - x_1)^2}{2\delta_{0x}^2} - \frac{(y_2 - y_1)^2}{2\delta_{0y}^2}\right] \times L_n^0 \left[\frac{(x_2 - x_1)^2}{2\delta_{0x}^2} + \frac{(y_2 - y_1)^2}{2\delta_{0y}^2} \right] \quad (1)$$

* Corresponding author.

** Corresponding author.

E-mail addresses: gqwang@dlmu.edu.cn (G. Wang), liudajun@dlmu.edu.cn (D. Liu).

where w_0 is the beam width; δ_{0x} and δ_{0y} are the coherence widths. In Eq. (1), L_n^0 is the Laguerre polynomial.

Considering the scheme of a radial PL beam array, and setting this beam array is composed of M beamlets, the center of random beamlet is located at (R_{mx}, R_{my}) and which is given as

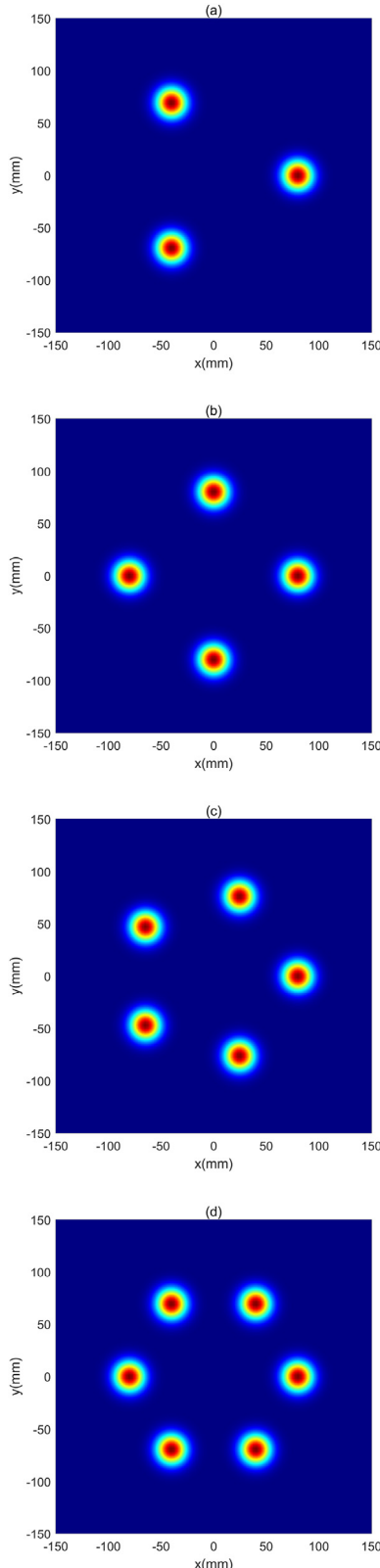


Figure 1. The intensity pattern of the radial PL circular LGCSM beam array at the source plane for the different M . (a) $M = 3$, (b) $M = 4$, (c) $M = 4$, (d) $M = 6$.

$$R_{mx} = R \cos \varphi_m \quad (2)$$

$$R_{my} = R \sin \varphi_m \quad (3)$$

$$\varphi_m = m \frac{2\pi}{M}, m = 1, 2, \dots, M \quad (4)$$

In Eqs. (2), (3), and (4), (R_{mx}, R_{my}) and φ_m are the center and phase of the beamlet.

Now we introduce the expression of a radial PL beam array composed of M elliptical LGCSM beamlets, the CSD of a radial PL elliptical LGCSM beam array can be expressed as

$$\begin{aligned} \Gamma_M(\mathbf{r}_1, \mathbf{r}_2, 0) = & \sum_{m=1}^M \sum_{h=1}^M \exp \left[-\frac{(x_1 - R_{mx})^2 + (y_1 - R_{my})^2}{4w_0^2} \right] \\ & \exp \left[-\frac{(x_2 - R_{hx})^2 + (y_2 - R_{hy})^2}{4w_0^2} \right] \quad \exp \left[-\frac{[(x_2 - R_{hx}) - (x_1 - R_{mx})]^2}{2\delta_{0x}^2} \right] \\ & \exp \left[-\frac{[(y_2 - R_{hy}) - (y_1 - R_{my})]^2}{2\delta_{0y}^2} \right] \\ & L_n^0 \left[\frac{[(x_2 - R_{hx}) - (x_1 - R_{mx})]^2}{2\delta_{0x}^2} + \frac{[(y_2 - R_{hy}) - (y_1 - R_{my})]^2}{2\delta_{0y}^2} \right]^q \\ & \times \exp[i(\varphi_m - \varphi_h)] \end{aligned} \quad (5)$$

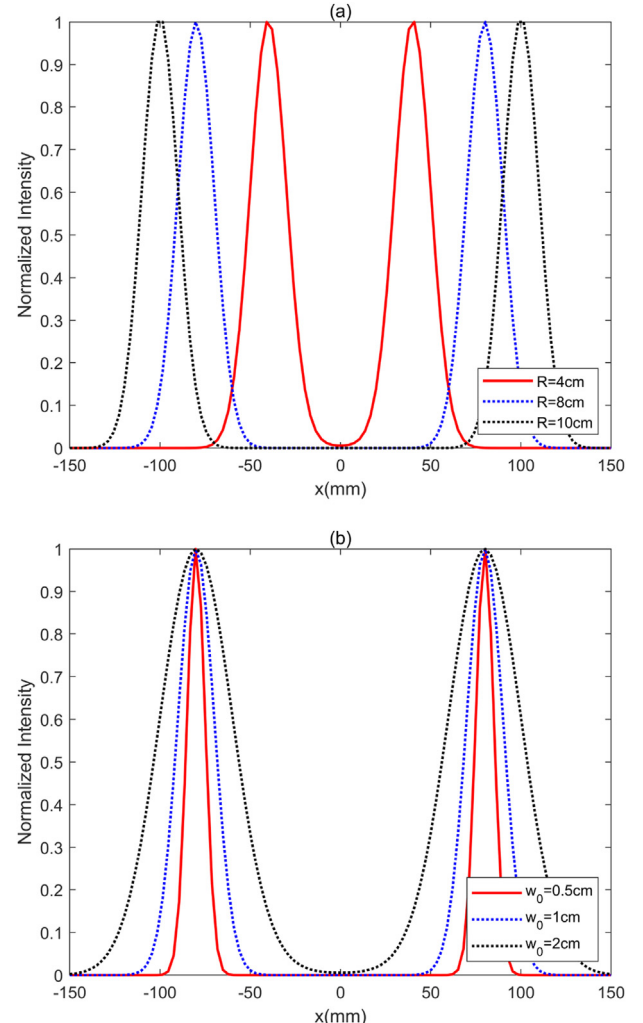


Figure 2. Cross-sections of intensity pattern of the radial PL circular LGCSM beam array with $M = 4$ at source plane. (a) different R , (b) different w_0 .

When $\delta_{0x} = \delta_{0y}$ in equation (5), a radial PL elliptical LGCSM beam array becomes radial PL circular LGCSM beam array. When $n = 0$, this beam array will reduce to a radial PL GSM beam array. Figure 1 shows the normalized intensity of a radial PL circular LGCSM beam array with $w_0 = 10\text{mm}$ and $R = 80\text{mm}$ for the different M ($M = 3$ in Figure 1a, $M = 4$ in Figure 1b, $M = 5$ in Figure 1c and $M = 6$ in Figure 1d). The cross-sections of a radial PL circular LGCSM beam array with $M = 4$ for the different R and w_0 are shown in Figure 2. As R increases, the distance between beamlets of this beam array will increase (Figure 2a). When R remains same, the widths of beamlets will increase as w_0 increases (Figure 2b). Thus, the intensity pattern of this beam array can be controlled by beam parameters R and w_0 .

Recalling the following equation [34].

$$L_n(x) = \sum_{q=0}^n \binom{n}{q} \frac{(-1)^q}{q!} x^q \quad (6)$$

$$(x^2 + y^2)^p = \sum_{m=0}^p \binom{p}{m} x^{2(p-m)} y^{2m} \quad (7)$$

Substituting Eqs. (6) and (7) into Eq. (5), the CSD of a radial PL elliptical LGCSM beam array can be rewritten as

$$\begin{aligned} \Gamma_M(\mathbf{r}_1, \mathbf{r}_2, 0) &= \sum_{m=1}^M \sum_{h=1}^M \exp[i(\varphi_m - \varphi_h)] \sum_{q=0}^n \binom{n}{q} \frac{(-1)^q}{q!} \\ &\quad \sum_{p=0}^q \binom{q}{p} \frac{1}{(\sqrt{2} \delta_{0x})^{2(q-p)}} \frac{1}{(\sqrt{2} \delta_{0y})^{2p}} \\ &\quad \times \exp \left[-\frac{(x_1 - R_{mx})^2 + (y_1 - R_{my})^2}{4w_0^2} \right] \exp \left[-\frac{(x_2 - R_{hx})^2 + (y_2 - R_{hy})^2}{4w_0^2} \right] \\ &\quad \times \exp \left[-\frac{[(x_2 - R_{hx}) - (x_1 - R_{mx})]^2}{2\delta_{0x}^2} \right] \exp \left[-\frac{[(y_2 - R_{hy}) - (y_1 - R_{my})]^2}{2\delta_{0y}^2} \right] \end{aligned} \quad (8)$$

3. Propagation of an LGCSM beam array

When a radial PL LGCSM beam array propagates through free space, the CSD of this beam array can be written by the extended Huygens-Fresnel principle [5, 6, 7, 8, 9, 10, 11, 12, 13, 14, 15, 16, 17, 18, 19, 20, 21].

$$\begin{aligned} \Gamma_M(\mathbf{p}_1, \mathbf{p}_2, z) &= \frac{k^2}{4\pi^2 z^2} \int_{-\infty}^{+\infty} \int_{-\infty}^{+\infty} \int_{-\infty}^{+\infty} \int_{-\infty}^{+\infty} \Gamma_M(\mathbf{r}_1, \mathbf{r}_2, 0) \\ &\quad \times \exp \left[-\frac{ik}{2z} (\mathbf{p}_1 - \mathbf{r}_1)^2 + \frac{ik}{2z} (\mathbf{p}_2 - \mathbf{r}_2)^2 \right] d\mathbf{p}_1 d\mathbf{p}_2 \end{aligned} \quad (9)$$

with $k = 2\pi/\lambda$, and λ is the wavelength.

Recalling the following equations [34].

$$\int_{-\infty}^{+\infty} x^n \exp(-ax^2 + 2bx) dx = \sqrt{\frac{\pi}{a}} \left(\frac{i}{2\sqrt{a}} \right)^n \exp \left(\frac{b^2}{a} \right) H_n \left(-\frac{ib}{\sqrt{a}} \right) \quad (10)$$

$$H_n(x) = \sum_{l=0}^{\left[\frac{n}{2}\right]} \frac{(-1)^l n!}{l!(n-2l)!} (2x)^{n-2l} \quad (11)$$

On substituting Eq. (8) into (9) and considering Eqs. (10) and (11), the CSD of a radial PL LGCSM beam array in free space is get as

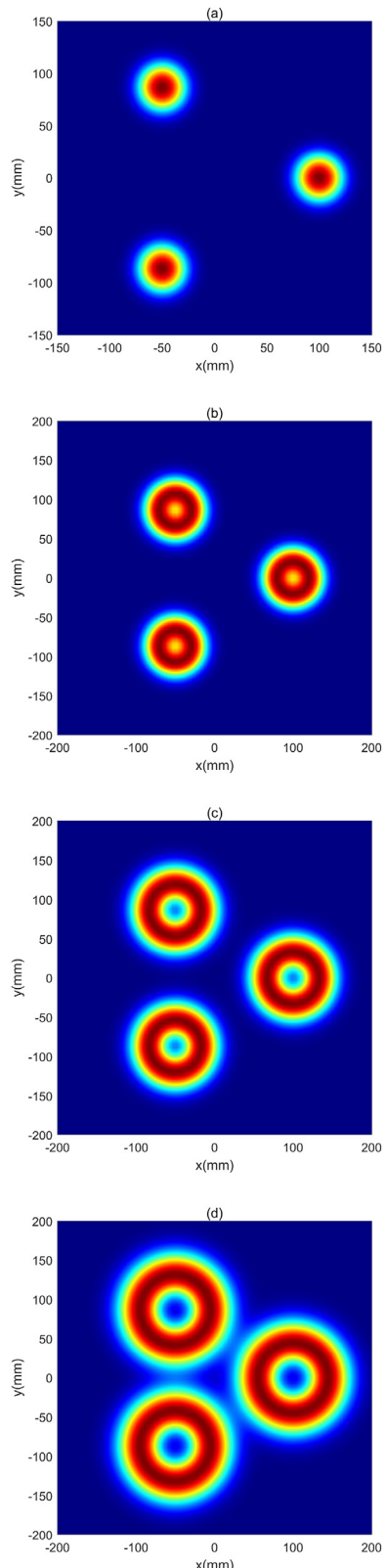


Figure 3. The normalized intensity of the radial PL circular LGCSM beam array with $M = 3$ at several distances. (a) $z = 100\text{m}$, (b) $z = 200\text{m}$, (c) $z = 300\text{m}$, (d) $z = 400\text{m}$.

$$\begin{aligned} \Gamma_M(\rho_1, \rho_2, z) = & \frac{k^2}{4\pi^2 z^2} \exp\left(-\frac{ik}{2z}\rho_1^2 + \frac{ik}{2z}\rho_2^2\right) \\ & \times \sum_{m=1}^M \sum_{h=1}^M \exp[i(\varphi_m - \varphi_h)] \sum_{q=0}^n \binom{n}{q} \frac{(-1)^q}{q!} \sum_{p=0}^q \binom{q}{p} \frac{1}{(\sqrt{2}\delta_{0x})^{2(q-p)}} \frac{1}{(\sqrt{2}\delta_{0y})^{2p}} \\ & \times S(\rho_x, z)S(\rho_y, z) \end{aligned} \quad (12)$$

with

$$\begin{aligned} S(\rho_x, z) = & \exp\left[-\frac{ik}{2z}(R_{mx}^2 - R_{hx}^2)\right] \exp\left[\frac{ik}{z}(\rho_{1x}R_{mx} - \rho_{2x}R_{hx})\right] \\ & \sum_{s_x=0}^{2(q-p)} \frac{(2q-2p)!(-1)^{s_x}}{s_x!(2q-2p-s_x)!} \sqrt{\frac{\pi}{a_x}} s_x! \left(\frac{1}{a_x}\right)^{s_x} \\ & \exp\left[\frac{1}{a_x}\left(-\frac{ik}{2z}R_{mx} + \frac{ik}{2z}\rho_{1x}\right)^2\right] \sum_{t_x=0}^{\lfloor \frac{s_x}{2} \rfloor} \frac{1}{t_x!(s_x-2t_x)!} \left(\frac{a_x}{4}\right)^{t_x} \end{aligned} \quad (13)$$

$$\sum_{d_x=0}^{s_x-2t_x} \frac{(s_x-2t_x)!}{d_x!(s_x-2t_x-d_x)!} \left(-\frac{ik}{2z}R_{mx} + \frac{ik}{2z}\rho_{1x}\right)^{s_x-2t_x-d_x} \left(\frac{1}{2\delta_{0x}^2}\right)^{d_x}$$

$$\sqrt{\frac{\pi}{b_x}} \left(\frac{i}{2\sqrt{b_x}}\right)^{2(q-p)-s_x+d_x} \exp\left(\frac{c_x^2}{b_x}\right) H_{2(q-p)-s_x+d_x}\left(-\frac{ic_x}{\sqrt{b_x}}\right)$$

$$S(\rho_y, z) = \exp\left[-\frac{ik}{2z}(R_{my}^2 - R_{hy}^2)\right] \exp\left[\frac{ik}{z}(\rho_{1y}R_{my} - \rho_{2y}R_{hy})\right]$$

$$\sum_{s_y=0}^{2p} \frac{(2p)!(-1)^{s_y}}{s_y!(2p-s_y)!} \sqrt{\frac{\pi}{a_y}} s_y! \left(\frac{1}{a_y}\right)^{s_y}$$

$$\exp\left[\frac{1}{a_y}\left(-\frac{ik}{2z}R_{my} + \frac{ik}{2z}\rho_{1y}\right)^2\right] \sum_{t_y=0}^{\lfloor \frac{s_y}{2} \rfloor} \frac{1}{t_y!(s_y-2t_y)!} \left(\frac{a_y}{4}\right)^{t_y} \quad (14)$$

$$\sum_{d_y=0}^{s_y-2t_y} \frac{(s_y-2t_y)!}{d_y!(s_y-2t_y-d_y)!} \left(-\frac{ik}{2z}R_{my} + \frac{ik}{2z}\rho_{1y}\right)^{s_y-2t_y-d_y} \left(\frac{1}{2\delta_{0y}^2}\right)^{d_y}$$

$$\sqrt{\frac{\pi}{b_y}} \left(\frac{i}{2\sqrt{b_y}}\right)^{2p-s_y+d_y} \exp\left(\frac{c_y^2}{b_y}\right) H_{2p-s_y+d_y}\left(-\frac{ic_y}{\sqrt{b_y}}\right)$$

$$a_\beta = \frac{1}{4w_0^2} + \frac{1}{2\delta_{0\beta}^2} + \frac{ik}{2z} (\beta = x, y) \quad (15)$$

$$b_\beta = \frac{1}{4w_0^2} + \frac{1}{2\delta_{0\beta}^2} - \frac{ik}{2z} - \frac{1}{a_\beta} \left(\frac{1}{2\delta_{0\beta}^2} + \frac{1}{\rho_0^2}\right)^2 \quad (16)$$

$$c_\beta = \frac{ik}{2z} R_{h\beta} - \frac{ik}{2z} \rho_{2\beta} + \frac{1}{a_\beta} \left(\frac{1}{2\delta_{0\beta}^2}\right) \left(-\frac{ik}{2z} R_{m\beta} + \frac{ik}{2z} \rho_{1\beta}\right) \quad (17)$$

The intensity of a radial PL LGCSM beam array at plane z is given as [35].

$$I(\rho, z) = \Gamma_M(\rho, \rho, z) \quad (18)$$

4. Numerical simulations and discussions

By using Eqs. (12), (13), (14), (15), (16), (17), and (18), the evolutions of intensity distributions of a radial PL LGCSM beam array composed of M beamlets in free space are illustrated and analyzed. The parameters about the radial PL LGCSM beam array in numerical simulation are $\lambda = 532\text{nm}$, $w_0 = 10\text{mm}$, $R = 100\text{mm}$ and $n = 2$. The intensity

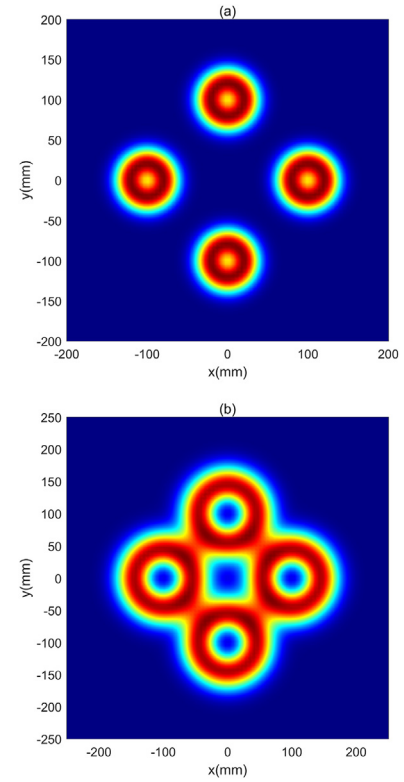


Figure 4. The normalized intensity of the radial PL circular LGCSM beam array with $M = 4$ at several distances. (a) $z = 200\text{m}$, (b) $z = 400\text{m}$.

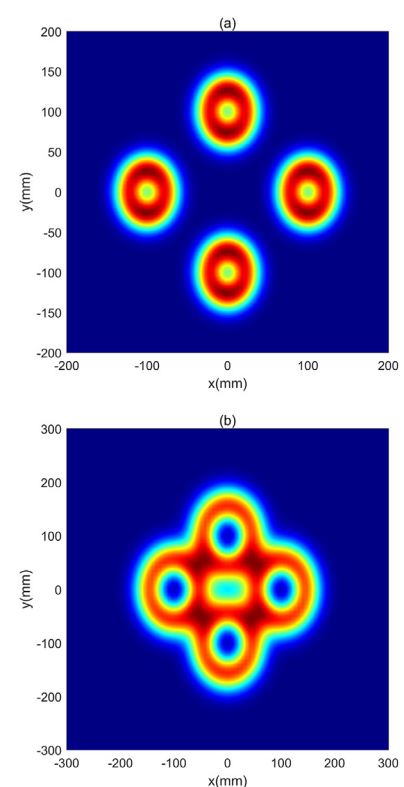


Figure 5. The normalized intensity of the radial PL elliptical LGCSM beam array with $M = 4$ at several distances. (a) $z = 200\text{m}$, (b) $z = 400\text{m}$.

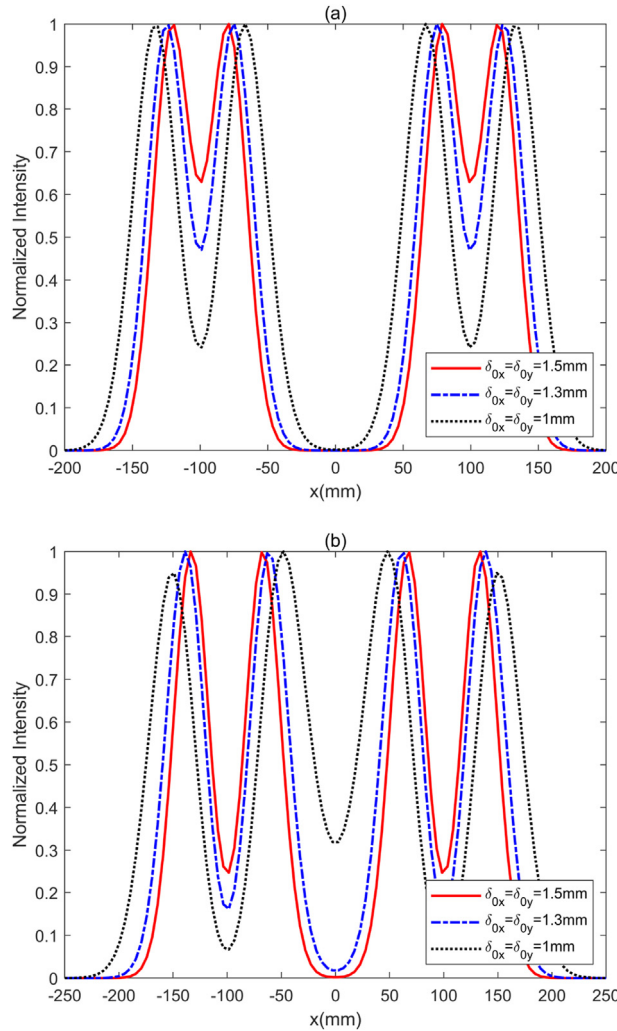


Figure 6. Cross-sections of intensity pattern of the radial PL circular LGCSM beam array with $M = 4$ for the different $\delta_{0x} = \delta_{0y}$ at several distances. (a) $z = 200m$, (b) $z = 300m$.

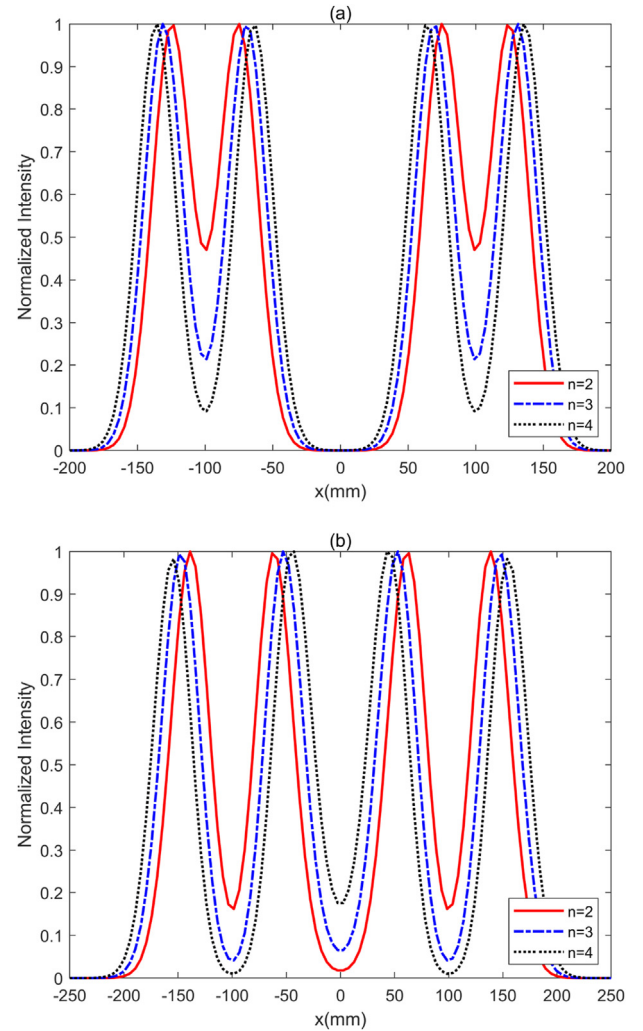


Figure 7. Cross-sections of intensity pattern of the radial PL circular LGCSM beam array with $M = 4$ for the different n at several distances. (a) $z = 200m$, (b) $z = 300m$.

profile of a radial PL circular LGCSM beam array with $M = 3$ and $\delta_{0x} = \delta_{0y} = 1.5mm$ propagating through free space at several distances are shown in Figure 3. Comparing Figure 1 with 3, it is seen that beamlets of this beam array can remain the initial Gaussian distribution (Figure 3a); the larger the distance is, the beamlet will gradually become a beam with ring pattern, while intensity at center of the beamlet is not zero (Figure 3b); As the distance increases further, the beamlets will translate into a dark hollow center beam, and the beam array has translated into a beam array composed of three circular LGCSM beams (Figures 3c and 3d). As M increases to $M = 4$ (Figure 4), the radial PL circular LGCSM beam array with $M = 4$ and $\delta_{0x} = \delta_{0y} = 1.5mm$ has a similar evolution phenomenon with beam array with $M = 3$ (Figures 3b and 4a), and this beam array at a longer distance is composed of four circular LGCSM beams (Figure 4b). The phenomenon that the dark hollow center of beamlets is caused by LGCSM sources, the LGCSM beam will evolve into dark hollow beam profile on propagation [22].

When coherence length $\delta_{0x} \neq \delta_{0y}$, a radial PL elliptical LGCSM beam array with $M = 4$, $\delta_{0x} = 1.5mm$ and $\delta_{0y} = 1.2mm$ is illustrated in Figure 5. One sees that the radial PL elliptical LGCSM beam array will have similar evolution to the circular LGCSM beam array (Figures 4a and 5a). While, the radial PL elliptical LGCSM beam array with $\delta_{0x} = 1.5mm$ and $\delta_{0y} = 1.2mm$ will evolve into a beam array with four elliptical dark

hollow beams as distance increases (Figure 5b). Comparing Figures 3, 4, and 5, one can conclude that the intensity distribution of radial PL LGCSM beam array at the long distance can be controlled by setting different beam parameters M , δ_{0x} and δ_{0y} .

To view the influence of $\delta_{0x} = \delta_{0y}$ on intensity of the radial PL LGCSM beam array, Figure 6 gives the cross-sections of intensity of the radial PL circular LGCSM beam array with $M = 4$ for the different $\delta_{0x} = \delta_{0y}$. As distance increases to $z = 200m$ (Figure 6a), it is seen that the intensity of the dark center of beamlets for the circular LGCSM beam array with larger $\delta_{0x} = \delta_{0y}$ has larger intensity. Thus, the beamlets of a radial PL LGCSM beam array with smaller $\delta_{0x} = \delta_{0y}$ will evolve into LGCSM beams faster as distance increases (Figures 6a and 6b). So, the small coherence length $\delta_{0x} = \delta_{0y}$ is beneficial for radial PL LGCSM beam array evolving into beam array composed by the dark hollow beam profile.

The influences of order n of Laguerre polynomial on the evolution of intensity for the radial PL LGCSM beam array with $M = 4$ and $\delta_{0x} = \delta_{0y} = 1.3mm$ are illustrated in Figure 7. One can see that the beamlets of radial PL LGCSM beam array with larger n will translate into dark hollow center beams faster (Figure 7a at $z = 200m$, Figure 7b at $z = 300m$). Comparing Figure 6 with Figure 7, one can conclude that the intensity of the radial PL LGCSM beam array can be controlled by choosing distance z , coherence length and beam order n .

5. Conclusions

In summary, the new type beam array named the radially PL LGCSM beam array is introduced, the intensity distribution of this beam array has radial distribution. The CSD of such beam array propagating through free space are derived. The effects of beam parameters on intensity of such beam are studied during propagation. It is found that such beam array will translate from a beam array composed of Gaussian intensity distribution into a beam array composed of M circular or elliptical dark hollow beam profile, and beamlets are LGCSM beams. Furthermore, the beamlets of radial PL LGCSM beam array with smaller $\delta_{0x} = \delta_{0y}$ and larger n will evolve into LGCSM faster as distance increases. The results are useful for laser shaping. Thus, this method provides a way for introducing a beam array with dark hollow beam profile, and using the similar process of derivation of radial PL LGCSM beam array, the rectangular or linear beam array composed by LGCSM beamlets can also be obtained.

Declarations

Author contribution statement

Yaotian Yan: Analyzed and interpreted the data; Wrote the paper.
 Guiqiu Wang: Conceived and designed the experiments; Analyzed and interpreted the data; Wrote the paper.
 Yan Yin; Hongmin Yin: Analyzed and interpreted the data.
 Yaochuan Wang: Contributed reagents, materials, analysis tools or data.
 Dajun Liu: Conceived and designed the experiments; Wrote the paper.

Funding statement

Professor Dajun Liu, Guiqiu Wang, Yaochuan Wang were supported by National Natural Science Foundation of China [11604038 & 11875096 & 11404048], and Financial support of Liaoning Provincial Department of Education [LJKZ0054].

Data availability statement

Data will be made available on request.

Declaration of interest's statement

The authors declare no conflict of interest.

Additional information

No additional information is available for this paper.

References

- [1] Y. Cai, Y. Chen, H.T. Eyyuboglu, Y. Baykal, Propagation of laser array beams in a turbulent atmosphere, *Appl. Phys. B* 88 (2007) 467–475.
- [2] H.T. Eyyuboglu, Y. Baykal, Y. Cai, Scintillations of laser array beams, *Appl. Phys. B* 91 (2008) 265–271.
- [3] P. Zhou, Z.J. Liu, X.J. Xu, X.X. Chu, Propagation of coherently combined flattened laser beam array in turbulent atmosphere, *Opt. Laser. Technol.* 41 (2009) 403–407.
- [4] L. Lu, X.L. Ji, X.Q. Li, J.P. Deng, H. Chen, T. Yang, Influence of oceanic turbulence on propagation characteristics of Gaussian array beams, *Optik* 125 (2014) 7154–7161.
- [5] F. Wang, X.L. Liu, Y.J. Cai, Propagation of partially coherent beam in turbulent atmosphere: a review, *Prog. Electromagn. Res.* 150 (2015) 123–143.
- [6] Y.B. Zhu, D.M. Zhao, X.Y. Du, Propagation of stochastic Gaussian-Schell model array beams in turbulent atmosphere, *Opt. Express* 16 (2008) 18437–18442.
- [7] X.L. Ji, X.L. Shao, Influence of turbulence on the beam propagation factor of Gaussian Schell-model array beams, *Opt. Commun.* 283 (2010) 869–873.
- [8] M. Sharifi, B. Luo, A.H. Dang, H. Guo, G.H. Wu, Spectral changes of a radial Gaussian schell-model beam array propagating in non-Kolmogorov turbulence, *J. Kor. Phys. Soc.* 63 (2013) 1925–1931.
- [9] Y. Zhang, T. Hou, Q. Chang, H. Chang, J. Long, P. Ma, P. Zhou, Propagation properties of Gaussian schell-model beam array in the jet engine exhaust induced turbulence, *IEEE Photonics J.* 12 (2020) 1–13.
- [10] Q.B. Suo, Y.P. Han, Z.W. Cui, Evolution properties of a Gaussian Schell-model Array beam in a uniaxial crystal orthogonal to the optical axis, *Optik* 176 (2019) 350–356.
- [11] Y.J. Cai, Q. Lin, Y. Baykal, H.T. Eyyuboglu, Off-axis Gaussian Schell-model beam and partially coherent laser array beam in a turbulent atmosphere, *Opt. Commun.* 278 (2007) 157–167.
- [12] Z. Mei, O. Korotkova, Sources for random arrays with structured complex degree of coherence, *Opt. Lett.* 43 (2018) 2676–2679.
- [13] Y. Zhou, D. Zhao, Statistical properties of electromagnetic twisted Gaussian Schell-model array beams during propagation, *Opt. Express* 27 (2019).
- [14] G.Q. Zhou, Propagation of a radial phased-locked Lorentz beam array in turbulent atmosphere, *Opt. Express* 19 (2011) 24699–24711.
- [15] B.B. Ma, C. Sun, X. Lv, J.B. Zhang, X.B. Yang, G.H. Wang, W.Y. Hong, D.M. Deng, Effect of turbulent atmosphere on the propagation of a radial phased-locked rotating elliptical Gaussian beam array, *J. Opt. Soc. Am. A* 36 (2019) 1690–1698.
- [16] D. Liu, Y. Wang, H. Zhong, Average intensity of radial phased-locked partially coherent standard Hermite-Gaussian beam in oceanic turbulence, *Opt. Laser. Technol.* 106 (2018) 495–505.
- [17] K.L. Wang, C.H. Zhao, Propagation properties of a radial phased-locked partially coherent anomalous hollow beam array in turbulent atmosphere, *Opt. Laser. Technol.* 57 (2014) 44–51.
- [18] D. Liu, H. Zhong, G. Wang, H. Yin, Y. Wang, Propagation of a radial phase-locked partially coherent elegant Laguerre-Gaussian beam array in non-Kolmogorov medium, *Appl. Phys. B* 125 (2019) 52.
- [19] L. Lu, Z. Wang, Y. Cai, Propagation properties of phase-locked radially-polarized vector fields array in turbulent atmosphere, *Opt. Express* 29 (2021) 16833–16844.
- [20] D. Liu, H. Zhong, G. Wang, H. Yin, Y. Wang, Radial phased-locked multi-Gaussian Schell-model beam array and its properties in oceanic turbulence, *Opt. Laser. Technol.* 124 (2020), 106003.
- [21] S. Zheng, J. Huang, X. Ji, K. Cheng, T. Wang, Rotating anisotropic Gaussian Schell-model array beams, *Opt. Commun.* 484 (2021), 126684.
- [22] Y.H. Chen, L. Liu, F. Wang, C.L. Zhao, Y.J. Cai, Elliptical Laguerre-Gaussian correlated schell-model beam, *Opt. Express* 22 (2014) 13975–13987.
- [23] Y.H. Chen, F. Wang, C.L. Zhao, Y.J. Cai, Experimental demonstration of a Laguerre-Gaussian correlated Schell-model vortex beam, *Opt. Express* 22 (2014) 5826–5838.
- [24] X. Peng, L. Liu, F. Wang, S. Popov, Y. Cai, Twisted Laguerre-Gaussian Schell-model beam and its orbital angular moment, *Opt. Express* 26 (2018) 33956–33969.
- [25] M. Luo, D. Zhao, Elliptical Laguerre Gaussian Schell-model beams with a twist in random media, *Opt. Express* 27 (2019) 30044–30054.
- [26] Y. Chen, J. Yu, Y. Yuan, F. Wang, Y. Cai, Theoretical and experimental studies of a rectangular Laguerre-Gaussian-correlated Schell-model beam, *Appl. Phys. B* 122 (2016) 31.
- [27] J. Zhao, G. Wang, Y. Yin, Y. Wang, H. Zhong, D. Liu, Propagation of a rectangular Laguerre-Gaussian correlated Schell-model beam in uniaxial crystal, *Optik* 241 (2021), 166495.
- [28] H.F. Xu, H.W. Wu, H.J. Chen, Z.Q. Sheng, J. Qu, Propagation properties of rectangular Laguerre-Gaussian-correlated Schell-model beams in atmospheric turbulence, *J. Mod. Opt.* 66 (2019) 208–217.
- [29] J.B. Su, C.A. Xu, H.F. Xu, J. Qu, Evolution properties of the radially polarized Laguerre-Gaussian-correlated Schell-model beams propagating in uniaxial crystals, *J. Opt. Soc. Am. A* 37 (2020) 529–539.
- [30] Y. Liu, R. Lin, F. Wang, Y. Cai, J. Yu, Propagation properties of Laguerre-Gaussian Schell-model beams with a twist phase, *J. Quant. Spectrosc. Radiat. Transf.* 264 (2021), 107556.
- [31] B. Yang, Y. Chen, F. Wang, Y. Cai, Trapping two types of Rayleigh particles simultaneously by a focused rotational elliptical Laguerre-Gaussian correlated Schell-model beam, *J. Quant. Spectrosc. Radiat. Transf.* 262 (2021), 107518.
- [32] H. Tang, B. Ou, Average spreading of a linear Gaussian-Schell model beam array in non-Kolmogorov turbulence, *Appl. Phys. B-Lasers Opt.* 104 (2011) 1007–1012.
- [33] X. Ma, D. Liu, Y. Wang, H. Yin, H. Zhong, G. Wang, Propagation of rectangular multi-Gaussian schell-model array beams through free space and non-Kolmogorov turbulence, *Appl. Sci.* 10 (2020) 450.
- [34] H.D.A. Jeffrey, *Handbook of Mathematical Formulas and Integrals*, fourth ed., Academic Press, 2008.
- [35] E. Wolf, Unified theory of coherence and polarization of random electromagnetic beams, *Phys. Lett.* 312 (2003) 263–267.